Comparative analysis of RNA enrichment methods for preparation of *Cryptococcus neoformans* RNA sequencing libraries

Calla L. Telzrow,[*,†] Paul J. Zwack,[‡] Shannon Esher Righi ,[§] Fred S. Dietrich,[†] Cliburn Chan,[**] Kouros Owzar,[,††] J. Andrew Alspaugh,[*,†] Joshua A. Granek[**,††,1]**

[*]Department of Medicine, Duke University School of Medicine, Durham, NC 27710,

[†]Department of Molecular Genetics and Microbiology, Duke University School of Medicine, Durham, NC 27710,

[‡]Department of Biology, Duke University, Durham, NC 27710,

[§]Department of Microbiology and Immunology, Tulane University School of Medicine, New Orleans, LA 70112,

[**]Department of Biostatistics and Bioinformatics, Duke University Medical Center, Durham, NC 27710,

[††]Duke Cancer Institute, Duke University, Durham, NC 27710

GitHub repositories:

https://github.com/granek/rna_enrichment

https://github.com/granek/LncPipe

GEO repository:

GSE160397

Running title:

Cryptococcus neoformans RNA enrichment methods

Keywords:

RNA sequencing, RNA enrichment, ribosomal RNA, non-coding RNA

[1] Corresponding author:

Joshua A. Granek

2424 Erwin Rd., 11099 Hock Plaza, Durham, NC 27710

Box 2721

(919) 684-0333

joshua.granek@duke.edu

ABSTRACT

Ribosomal RNA (rRNA) is the major RNA constituent of cells, therefore most RNA sequencing (RNA-Seq) experiments involve removal of rRNA. This process, called RNA enrichment, is done primarily to reduce cost: without rRNA removal, deeper sequencing would need to be performed to balance the sequencing reads wasted on rRNA. The ideal RNA enrichment method would remove all rRNA without affecting other RNA in the sample. We have tested the performance of three RNA enrichment methods on RNA isolated from *Cryptococcus neoformans*, a fungal pathogen of humans. We show that the RNase H depletion method unambiguously outperforms the commonly used Poly(A) isolation method: the RNase H method more efficiently depletes rRNA while more accurately recapitulating the expression levels of other RNA observed in an unenriched “gold standard”. The RNase H depletion method is also superior to the Ribo-Zero depletion method as measured by rRNA depletion efficiency and recapitulation of protein-coding gene expression levels, while the Ribo-Zero depletion method performs moderately better in preserving non-coding RNA (ncRNA). Finally, we have leveraged this dataset to identify novel long non-coding RNA (lncRNA) genes and to accurately map the *C. neoformans* mitochondrial rRNA genes.

ARTICLE SUMMARY

We compare the efficacy of three different RNA enrichment methods for RNA-Seq in *Cryptococcus neoformans*: RNase H depletion, Ribo-Zero depletion, and Poly(A) isolation. We show that the RNase H depletion method, which is evaluated in *C. neoformans* samples for the first time here, is highly efficient and specific in removing rRNA. Additionally, using data generated through these analyses, we identify novel long non-coding RNA genes in *C. neoformans*. We conclude that RNase H depletion is an effective and reliable method for preparation of *C. neoformans* RNA-Seq libraries.

INTRODUCTION

RNA sequencing (RNA-Seq) is a powerful tool for quantifying gene expression in diverse organisms. Despite the rapid and continual decrease in sequencing costs, the expense of sequencing is often the limiting factor in designing RNA-Seq experiments. Due to this cost constraint, enrichment of the RNA classes of interest, hereafter referred to as “RNA enrichment”, is an important step in library preparation for most RNA-Seq experiments. Ribosomal RNA (rRNA) is the most abundant RNA in any cell, generally constituting more than 90% of the total RNA (Giannoukos *et al.* 2012). Despite its abundance, it is rarely of interest in RNA-Seq experiments, therefore, 90% or more of the data is useless when generated without an RNA enrichment step. RNA enrichment aims to reduce the content of RNA in the library, eliminating sequencing capacity wasted on uninformative data and reducing the cost of data storage and analysis, thus decreasing the overall cost of the experiment.

There are many different methods for RNA enrichment and many products available based on these different methods. When selecting an RNA enrichment method and product there are two key considerations: 1) the fraction of rRNA removed; 2) the side effects on other RNAs in the sample. RNA enrichment methods either specifically target the RNA of interest, most commonly mRNA, for isolation or specifically target rRNA for removal (Zhao *et al.* 2014). The most common mRNA isolation method, poly(A) isolation, uses an oligo(dT) affinity matrix. Raw RNA is hybridized to the matrix, which preferentially binds the 3’ polyadenylation sequence of mRNA. By enriching polyadenylated mRNA, rRNA, which lacks 3’ polyadenylation, is depleted de facto. Although mRNA isolation methods are typically efficient in eliminating

rRNA, they fail to capture any RNA molecules lacking polyadenylation, such as non-coding RNA (ncRNA). They are also only applicable to eukaryotes, since mRNA in prokaryotes is generally not polyadenylated. Most rRNA removal methods involve hybridization of sequence-specific probes to rRNA. These probes target the rRNA for depletion. In the Ribo-Zero depletion method, the probes are synthesized with a molecular tag, which is used to bind the probe-rRNA complex to beads, allowing the complexed rRNA to be removed from solution (Zhao *et al.* 2014). In the ribonuclease H (RNase H) depletion method, sequence-specific DNA probes hybridized to rRNA target the rRNA for enzymatic degradation by RNase H, which specifically degrades RNA from RNA-DNA complexes (Morlan *et al.* 2012). The duplex-specific nuclease (DSN) method indiscriminately depletes high abundance sequences by denaturing and reannealing the prepared RNA-Seq library, then treating with a duplex-specific nuclease to degrade all double-stranded DNA. Under the conditions used for reannealing, high abundance sequences are much more likely to find a complementary sequence, so high abundance sequences, including but not limited to rRNA, are preferentially removed from the pool (Yi *et al.* 2011).

The poly(A) isolation and DSN methods are attractive because they are broadly applicable without any organism-specific adaptation: the poly(A) method works in all eukaryotes and the DSN method should work in any organism. However, the rRNA removal methods (Ribo-Zero and RNase H) are more targeted, and are therefore expected to have fewer side-effects on biologically-important RNA molecules, such as protein-coding RNA and ncRNA. The downside inherent in the targeted nature of the rRNA depletion methods is that the sequence-specific probes must be designed for the

organism under experimentation or a close relative for maximal efficacy. Because rRNA is the most highly conserved sequence across the tree of life (Isenbarger *et al.* 2008), probes designed for an evolutionarily distant species will often work, but efficiency of rRNA depletion decreases with evolutionary distance. For all rRNA depletion methods, the performance of these rRNA removal methods can vary by organism, so it is important to assess them on the organism of interest.

The budding yeast *Cryptococcus neoformans* is a human fungal pathogen that infects more than 200,000 people annually and causes excessive mortality among immunocompromised patient populations, such as those with HIV/AIDS and those receiving immunosuppressive cancer therapies (Rajasingham *et al.* 2017). Research on *C. neoformans* helps us better understand this pathogen, contributes to the development of treatments for *C. neoformans* infections, and advances our understanding of fungal pathogens in general. RNA-Seq has been used extensively in *C. neoformans* studies to elucidate regulatory networks of protein-coding genes (Chang *et al.* 2014; Chen *et al.* 2014; Janbon *et al.* 2014; Gish *et al.* 2016; Chow *et al.* 2017; Brown *et al.* 2018, 2020; Yu *et al.* 2020). While there is intense interest in the role of ncRNA in higher eukaryotes such as humans, relatively little work has explored the implications of ncRNA in fungi, with focus largely on model fungi such as *Saccharomyces cerevisiae* (Bird *et al.* 2006; Bumgarner *et al.* 2009, 2011; Gelfand *et al.* 2011; Parker *et al.* 2018) and *Schizosaccharomyces pombe* (Ding *et al.* 2012; Atkinson *et al.* 2018). However, multiple recent studies have demonstrated the importance of ncRNA in *Cryptococcus* biology and virulence, including microRNA (miRNA) (Jiang *et al.* 2012; Liu *et al.* 2020), small interfering RNA (siRNA) (Wang *et al.* 2010; Janbon *et al.*

2010; Liu *et al.* 2020), and long non-coding RNA (lncRNA) (Fan *et al.* 2005; Chacko *et al.* 2015; Liu *et al.* 2020).

In planning and analyzing RNA-Seq experiments in *C. neoformans*, it is essential to understand the side-effect profile of the RNA enrichment method used. RNA enrichment methods that alter levels of RNA of interest may give misleading or incorrect results; this is a special concern for analysis of ncRNA. Here, we assess three different enrichment methods for RNA-Seq applications in *C. neoformans*: RNase H depletion, Ribo-Zero depletion, and Poly(A) isolation. The Ribo-Zero depletion ("Ribo-Zero Kit Species Compatibility Tables"; Trevijano-Contador *et al.* 2018; Liu *et al.* 2020) and Poly(A) isolation (Bloom *et al.* 2019; Brown *et al.* 2020) methods have been used previously in *C. neoformans*, while the RNase H method has not. However, none of these methods have been evaluated in *C. neoformans* in comparison to each other, much less to an unenriched "gold standard." By performing this controlled experiment, we have been able to quantify the efficiency of rRNA depletion and determined the side-effects of each depletion method on non-rRNA genes.

We find that the RNase H depletion method is more efficient than the Ribo-Zero depletion and the Poly(A) isolation methods in removing rRNA. Additionally, we report that the RNase H depletion method is highly specific; it performs better than the other two methods in preserving protein-coding RNA, and nearly as well as the Ribo-Zero depletion method in preserving ncRNA. Because the RNase H depletion and Ribo-Zero depletion methods both preserve ncRNA, we utilized the data generated from these methods to identify novel *C. neoformans* lncRNA. Collectively, this work demonstrates that RNase H depletion is an effective RNA enrichment method for use in preparation of

179 *C. neoformans* RNA-Seq libraries, further emphasizes the role of RNA enrichment in
180 design of economical RNA-Seq experiments, and highlights the importance of knowing
181 the side-effect profile when choosing an RNA enrichment method.
182
183 **MATERIALS AND METHODS**
184 **Strains, media, and growth conditions:**
185 The *C. neoformans* var. *grubii* H99 (*MAT*α) wild-type strain was used for all
186 experiments. This strain was maintained on yeast extract-peptone-dextrose (YPD)
187 medium (1% yeast extract, 2% peptone, 2% dextrose, and 2% agar for solid medium).
188
189 **RNA-Seq library preparation:**
190 Three biological replicate samples (A, B, and C) were used for all analyses.
191 Samples were prepared by growing H99 to mid-logarithmic growth phase in three
192 separate flasks of liquid YPD medium, with 150 rpm shaking. Approximately
193 1×10^9 cells from each sample were pelleted, resuspended in fresh YPD medium, and
194 incubated at 30°C for 90 min with 150 rpm shaking. Cells were then pelleted, flash
195 frozen on dry ice, and lyophilized for ~18 hours. Total RNA was isolated using the
196 Qiagen RNeasy Plant Mini Kit (Qiagen, Valencia, CA); on-column DNase digestion was
197 performed to ensure elimination of contaminating genomic DNA. Total RNA quantity
198 and quality were assessed using the Agilent 2100 Bioanalyzer. Purified total RNA was
199 subsequently stored at -80°C.
200 Aliquots from each total RNA sample were treated with one of three different
201 RNA enrichment methods: the RNase H method for selective depletion of rRNA (Morlan

et al. 2012; Adiconis *et al.* 2013), the Ribo-Zero rRNA Removal Kit (Yeast) (Illumina, San Diego, CA), and the NEBNext® Poly(A) mRNA Magnetic Isolation Module (NEB #E7490) (New England Biolabs, Ipswich, MA). RNA-Seq libraries were prepared from these enriched samples and from unenriched control "gold standard" samples (i.e. "Unenriched") using the NEBNext® Ultra™ II Directional RNA Library Prep with Sample Purification Beads (NEB #E7765) and NEBNext® Multiplex Oligos for Illumina® (Dual Index Primers Set 1) (NEB #E7600) (New England Biolabs, Ipswich, MA). Libraries were pooled and sequenced by the Duke Sequencing and Genomic Technologies Shared Resource on an Illumina NextSeq 500 using the High-Output Kit to produce 75-basepair single-end reads.

It should be noted that while all work was done with the same three total RNA samples, the enrichment, library preparation, and sequencing were done in two batches, approximately one year apart. In between, total RNA samples were stored at -80°C. Ribo-Zero-treated, Poly(A)-treated, and Unenriched RNA control libraries were prepared and sequenced in the first batch. RNase H-treated, replicate Poly(A)-treated, and replicate Unenriched RNA control libraries were prepared and sequenced in the second batch. All Unenriched RNA samples were compared and shown to be highly correlated (Figures 2A, 3A, & 4A), demonstrating that batch effect and differences in total RNA storage times did not confound comparisons. It should also be noted that the Ribo-Zero-treated libraries, the Poly(A)-treated libraries, and the Unenriched libraries were prepared by multiple individuals, which may explain some of the sample variation within those groups, while the RNase H-treated libraries were all prepared by a single

224 individual. The individual who prepared each library is noted in the library metadata
225 deposited at GEO.
226
227 **RNase H depletion:**
228 The RNase H depletion method (Morlan *et al.* 2012; Adiconis *et al.* 2013) is
229 described briefly here; a more detailed protocol is included in supplementary data (File
230 S1). The hybridization reaction mixture consisted of 1 µg of total RNA, 1 µl of 5x
231 Hybridization Buffer (1000 mM NaCl, 500 mM Tris-HCl, pH 7.5), 0.65 µl of 100 µM
232 pooled targeting oligos (discussed below), and nuclease-free water to bring the reaction
233 to 5 µl. Oligo hybridization was performed in a thermocycler with the following program:
234 2 minutes at 95°C, ramp from 95°C to 22°C at -0.1°C/s, 5 minutes at 22°C. After
235 hybridization, samples were transferred to ice and RNase H (New England Biolabs,
236 Ipswich, MA) was added: 2 µl RNase H (5 U/µl), 1 µl 10x RNase H Reaction Buffer, 2 µl
237 nuclease-free water. RNase H digestion was performed at 37°C for 30 minutes. After
238 RNase H digestion, samples were stored on ice while adding DNase I (New England
239 Biolabs, Ipswich, MA): 4 µl DNase I (2 U/µl), 10 µl 10x DNase I Reaction Buffer, 76 µl
240 nuclease-free water. DNase I digestion was performed at 37°C for 30 minutes. After
241 DNase I digestion, samples were transferred to ice. rRNA depleted RNA was purified
242 from the reaction mixture with the Zymo RNA Clean & Concentrator-5 kit (Zymo
243 Research, Irvine, CA) according to manufacturer instructions and eluted in 12 µl
244 nuclease-free water. Finally, 5 µl of the eluted RNA was input to the library prep using
245 NEBNext® Ultra II Directional RNA Library Prep Kit for Illumina (New England Biolabs,
246 Ipswich, MA).

Analysis overview:

All genomic analyses used genome build CNA3 of H99 *Cryptococcus neoformans* var. *grubii* (accession GCA_000149245.3). The genome sequence and annotation were downloaded from release 39 of the Ensembl Fungi database (Kersey *et al.* 2016). For mapping mitochondrial rRNA genes, the original GTF downloaded from Ensembl Fungi was used. For all subsequent analyses, a modified GTF was used which included the newly mapped mitochondrial rRNA genes.

Analysis was performed using scripts written in the R programming language, Bash, and publicly available software detailed below. Custom R scripts used the following R and Bioconductor packages: Biostrings, BSgenome, dplyr, foreach, fs, GenomicAlignments, GenomicFeatures, ggbio, ggplot2, ggpubr, gridExtra, here, knitr, magrittr, plyr, readr, rmarkdown, Rsamtools, rstatix, rtracklayer, R.utils, stringr, tibble, tidyr, tools, utils.

Mapping of mitochondrial rRNA genes:

Coverage depth was plotted for all reads mapped to the mitochondrial chromosome for data generated from the first batch of Unenriched libraries. Visual inspection of these plots clearly indicated two regions with coverage depth several orders of magnitude higher than the rest of the chromosome. These regions do not overlap with any annotated feature in the mitochondrial chromosome. We determined the boundaries of these regions, extracted the sequences of the putative rRNA genes, and confirmed by BLASTn (Altschul *et al.* 1990) that these regions were homologous to

known fungal mitochondrial small (positions 16948-18316) and large (positions 6710-9326) subunit rRNA genes (Figure S1). A modified version of the *C. neoformans* genome annotation supplemented with our mitochondrial rRNA gene annotations is included (File S2).

Design of rRNA targeting oligonucleotides:

Short DNA oligos were designed to target all nuclear rRNA genes (CNAG_10500, CNAG_10501, CNAG_10502, CNAG_10503) and the newly annotated 15S and 21S rRNA mitochondrial genes. In order to guide degradation of all rRNA by RNase H, the DNA oligos must be complementary to the rRNA and completely tile the rRNA. For simplicity and cost minimization, the design goal for rRNA targeting oligos was for them to be 50 nucleotides in length with no gaps between adjacent oligos. For genes with lengths that were not multiples of 50 nucleotides, single nucleotide gaps were introduced between oligos to allow for end-to-end coverage. Two, 55 nucleotide oligos were used to tile CNAG_10503, which is 111bp long.

Oligos were validated by mapping them to the H99 genome and confirming that they tiled as expected and mapped to the antisense strand. This validation process identified several partial duplications of the mitochondrial rRNA, putative nuclear mitochondrial DNA (numts) (Hazkani-Covo *et al.* 2010), and nuclear rRNA. These duplications were found in CNAG_04124, CNAG_06164, CNAG_07466, CNAG_12145, CNAG_12438, CNAG_13073, and in the region between CNAG_10503 and CNAG_03595. CNAG_13073 was excluded from analysis of rRNA depletion specificity because the rRNA duplication it contains is in an exon and on the sense strand,

meaning that reads originating from rRNA genes can be misassigned to CNAG_13073. The other duplications do not result in spurious counts because they are either not in an exon or inserted antisense relative to the "host" gene.

The code used to design oligos should be applicable to other genomes; it is located within the file generate_rnaseh_oligos.Rmd, which is available, as described below, with the rest of the software developed for this project. This Rmarkdown document generates a TSV file in the correct format for pasting into the ordering template supplied by Eurofins; we have included a copy of the TSV generated for this project as a supplementary file (File S3). The 179 oligos were ordered from Eurofins Genomics LLC at a 10 nmol synthesis scale, with salt-free purification, resuspended to 100 µM, and shipped on dry ice. Upon receipt, all oligos were thawed, pooled, aliquoted, and stored at -80°C. Total cost for oligos (not including shipping) was less than $1000. This provided over 21 mL of pooled oligos (179 oligos at 120 µL per oligo), enough for over 33,000 reactions. Therefore, while the upfront cost of oligos is substantial, the per reaction cost is about $0.03.

Bioinformatics and statistical data analyses:

Basic assessments of sequence data quality were performed using FastQC (Andrews 2010) and MultiQC (Ewels *et al.* 2016). Raw sequencing reads were trimmed and filtered using fastq-mcf (EA-Utils version 1.04.807) (Aronesty 2011) and adapter sequences were extracted from the manufacturer-provided "Sample Sheet NextSeq E7600" template for the NEBNext® Multiplex Oligos for Illumina® (Dual Index Primers Set 1) (https://www.neb.com/tools-and-resources/usage-guidelines/sample-sheet-

nextseq-e7600, accessed 11/10/2020). Reads were then mapped to the genome and read counts were generated using STAR (version 2.5.4b) (Dobin *et al.* 2013). For quantification of reads mapped to genes, we use the fourth column ("counts for the 2nd read strand aligned with RNA") of the STAR ReadsPerGene.out.tab because the NEBNext® Ultra™ II Directional RNA Library Prep uses the dUTP method for strand-specific library preparation. All sequencing was done on an Illumina NextSeq 500, which has a flow cell with four lanes that are fluidically-linked (i.e., one pool is simultaneously loaded onto all four lanes). While we expect there to be some lane effects, we expect these to be less than fluidically-independent lanes. Because of this, and for simplicity, reads were combined across all four lanes for analysis of depletion efficiency and specificity.

Analysis of rRNA depletion efficiency:

To calculate the percentage of rRNA reads per library, Rsamtools (version 2.2.2) was used to extract reads from the STAR generated BAM files and determine the number of reads mapped to the rRNA genes. We did not use rRNA counts generated by STAR because STAR excludes multimapping reads from per gene read counts. As discussed above, several rRNA genes are partially duplicated elsewhere in the genome. Because STAR excludes multimapping reads from gene counts, it undercounts reads mapping to the rRNA genes that are partially duplicated. We confirmed the source of reads that mapped to rRNA duplicated regions by evaluating context: the count level of these reads corresponded to the level of expression of the rRNA genes from which the duplications seem to have arisen and not the level of expression of the genes (or

339 genomic region in the case of the partial duplication of CNAG_10500) that seem to be
340 the “acceptor sites” of these duplications. The percentage of total reads that mapped to
341 rRNA genes was then calculated.
342
343 **Enrichment correlation analyses:**
344 Per gene read counts were generated by STAR as described above. Read
345 counts for each library were combined across all four lanes using
346 DESeq2::collapseReplicates, each library’s counts were normalized by its size factor,
347 then an average count per gene was calculated for each enrichment method across all
348 replicates. The mean normalized count of the Unenriched replicate libraries was
349 considered the “gold standard” count for each gene. Specificity of each enrichment
350 method was determined by calculating the Pearson correlation of the mean normalized
351 count for each enrichment method with the Unenriched gold standard. Variation among
352 the Unenriched libraries was quantified by cross-correlation: Pearson correlation was
353 calculated for each Unenriched replicate library with the normalized mean of the other
354 five Unenriched replicate libraries. Scatterplots were generated to visualize the
355 correlation of replicate enriched libraries with the Unenriched gold standard. While
356 calculation of mean normalized counts used all replicates for each method, scatterplots
357 are only shown for one technical replicate of each RNA sample for each enrichment
358 method. In addition to analyses across all genes, calculation of Pearson correlation and
359 generation of scatterplots was repeated for subsets of genes, as annotated for
360 “gene_biotype”: protein-coding genes, ncRNA, and tRNA, according to each gene’s

annotation. rRNA genes and CNAG_13073 were excluded from all correlation analyses and scatterplots.

To determine specifically which genes seem to be "lost" by the Poly(A) isolation method, we identified genes with counts at least eight-fold lower in the Poly(A)-treated libraries than in the Unenriched libraries, after first excluding genes with very low expression in the Unenriched libraries (genes with less than 50 total read counts across all Unenriched libraries). These thresholds were chosen to identify obvious outliers in the Poly(A)-treated libraries, and were confirmed by visual inspection of the identified genes (Figure S6). We selected these thresholds to be more conservative than thresholds commonly used to identify genes with biologically relevant differences in expression (total reads of at least 10 and fold change of at least 2).

LncRNA analysis:

To identify novel lncRNA, we applied LncPipe (Zhao *et al.* 2018) to the data generated from the RNase H and Ribo-Zero enriched libraries and the Unenriched RNA libraries; Poly(A) enriched libraries were not included because they were expected to contain few, if any, reads derived from lncRNA. The published version of LncPipe only appears to work with data generated from human samples, so we forked the LncPipe repository and modified it to enable analysis of *C. neoformans* data. Details of the forked repository are provided below.

We developed an Rmarkdown document to perform all necessary pre-processing for running LncPipe (Zhao *et al.* 2018). This pre-processing involved automated reformatting of the input GTF file, preparing a subset of the GTF containing only protein-

coding genes and another subset containing only non-protein-coding genes, generating a *C. neoformans* specific model for CPAT (one component of LncPipe), and generating a Bash script which itself runs LncPipe. LncPipe itself was run in Singularity with the bioinformatist/lncpipe Docker image built by the LncPipe developers (https://hub.docker.com/layers/bioinformatist/lncpipe/latest/images/sha256-9d97261556d0a3b243d4aa3eccf4d65e458037e31d9abb959f84b6fe54bb99a2?context=explore). Within LncPipe, STAR was used for mapping reads and the file step, LncPipeReporter, was not run.

Data and reagent availability:

The RNA-Seq data analyzed in this publication have been deposited in NCBI's Gene Expression Omnibus (GEO) (Edgar *et al.* 2002) and will be accessible through GEO Series accession number GSE160397 (https://www.ncbi.nlm.nih.gov/geo/query/acc.cgi?acc=GSE160397). The custom programs developed for processing and analyzing the RNA-Seq data are available in a GitHub repository (https://github.com/granek/rna_enrichment) and the version of the LncPipe pipeline that we modified to run on the H99 genome is available in a GitHub repository (https://github.com/granek/LncPipe) that was forked from the original. For purposes of reproducibility, all analyses were run within Singularity containers (v 3.5.2). All lncRNA discovery was performed using the bioinformatist/lncpipe Docker image (run within Singularity) provided by the LncPipe developers (https://hub.docker.com/layers/bioinformatist/lncpipe/latest/images/sha256-9d97261556d0a3b243d4aa3eccf4d65e458037e31d9abb959f84b6fe54bb99a2?context

=explore). All other analyses were performed using a Singularity image which we built and is publicly available (library://granek/published/rna_enrichment). These resources include all programs, support files, and instructions for automatically replicating all analyses presented here using the data available from GEO.

Figure S1 contains a depth of coverage plot of the mitochondrial rRNA genes. Figures S2, S3, and S4 display scatterplot visualizations of rRNA depletion specificity summarized in Figures 2, 3, and 4, respectively. Figure S5 displays the rRNA depletion efficiency for ncRNA genes, excluding CNAG_12993. Figure S6 displays a scatterplot visualization of the genes that are underrepresented by the Poly(A) isolation method and Table S1 provides details of these genes. File S1 contains the RNase H depletion protocol. File S2 contains the Ensembl GTF with newly annotated mitochondrial rRNA. File S3 contains DNA oligonucleotide sequences used in the RNase H depletion method. All supplementary information has been deposited in figshare.

RESULTS

RNase H depletion is most efficient in removing rRNA:

We focus the majority of our analyses on the RNase H depletion and Poly(A) isolation methods, because, of the three RNA enrichment methods assessed here, they are the two that are still available for use. To provide some context to our RNase H depletion method results, we also include analyses on the Ribo-Zero depletion method, which was frequently used in fungal RNA-Seq experiments before its discontinuation.

As an initial assessment, we evaluated the efficiency with which each enrichment method removed rRNA. To do so, we quantified the percentage of total reads that

mapped to rRNA genes for each method and compared these percentages to those of Unenriched RNA control libraries generated by sequencing identical RNA samples without any enrichment. As expected, the vast majority (~90-92%) of reads in the Unenriched RNA control libraries map to rRNA genes (Figure 1). Both the RNase H-treated libraries (~1.5-2.5%) and the Poly(A)-treated libraries (~3-5%) display a significant reduction in the percentage of reads mapping to rRNA genes (Figure 1). The Ribo-Zero depletion method was previously demonstrated to be efficient in depleting fungal rRNA and was used successfully in RNA-Seq applications for various fungi (Illumina; Trevijano-Contador *et al.* 2018; Liu *et al.* 2020). We similarly evaluated the Ribo-Zero depletion method and observed that the number of mapped rRNA reads is significantly higher in the Ribo-Zero-treated libraries (~21-85%) than in the RNase H-treated and Poly(A)-treated libraries (Figure 1). Overall, both the RNase H depletion and Poly(A) isolation methods demonstrate robust efficiency in removing fungal rRNA, with the RNase H depletion method modestly outperforming the commonly-used Poly(A) isolation method.

RNase H depletion more accurately preserves true levels of non-rRNA than Poly(A) isolation:

To compare the specificity of the three RNA enrichment methods, we determined the correlation between read counts in the enriched libraries to read counts in the Unenriched RNA control libraries generated from the same samples. To do so, we first calculated the correlation coefficient between normalized reads mapped to all non-rRNA genes from all Unenriched RNA samples, in order to determine the maximum

453 achievable correlation between libraries. As expected, we observed that the Unenriched
454 RNA samples are highly correlated (R = 0.983-0.997), demonstrating reproducibility
455 between samples and batches (Figure 2A).

456 We compared the abilities of the RNase H depletion method and the Poly(A)
457 isolation method to preserve all non-rRNA following rRNA depletion. To do so, we
458 calculated the correlation coefficient between normalized reads mapped to all non-rRNA
459 genes in RNase H-treated/Poly(A)-treated libraries and normalized reads mapped to all
460 non-rRNA genes from the Unenriched RNA control libraries. We found that the RNase
461 H-treated libraries (R = 0.974-0.982) display a much better correlation with the
462 Unenriched RNA control libraries than the Poly(A)-treated libraries (R = 0.793-0.820) for
463 all reads mapping to non-rRNA genes (Figures 2B & S2). We similarly assessed the
464 Ribo-Zero depletion method for preservation of all non-rRNA. Ribo-Zero-treated libraries
465 (R = 0.932-0.954) display a much better correlation with the Unenriched libraries than
466 the Poly(A)-treated libraries, but a slightly weaker correlation than the RNase H-treated
467 libraries for reads mapping to all non-rRNA genes (Figure 2B & S2). This observation
468 suggests that the RNase H depletion method may be more specific than the Poly(A)
469 isolation and the Ribo-Zero depletion methods, in that it maintains non-rRNA levels
470 observed in the Unenriched RNA control libraries.
471
472 **RNase H depletion more accurately preserves true levels of protein-coding RNA**
473 **than Poly(A) isolation:**
474 We next assessed the ability of each RNA enrichment method to retain protein-
475 coding RNA specifically. To do so, we calculated the correlation coefficient between

476 normalized reads mapped to protein-coding genes from all Unenriched RNA samples, in
477 order to determine the maximum achievable correlation between libraries. As expected,
478 we observed that the Unenriched RNA samples are highly correlated (R = 0.986-0.998),
479 demonstrating reproducibility between samples and batches (Figure 3A).
480 We compared the ability of the RNase H depletion method and the Poly(A)
481 isolation method to preserve protein-coding RNA following rRNA depletion. To do so,
482 we calculated the correlation coefficient between normalized reads mapped to protein-
483 coding genes in RNase H-treated/Poly(A)-treated libraries and normalized reads
484 mapped to protein-coding genes from the Unenriched RNA control libraries. We found
485 that the RNase H-treated libraries (R = 0.985-0.990) display a much better correlation
486 with the Unenriched RNA control libraries than the Poly(A)-treated libraries (R = 0.810-
487 0.838) for all reads mapping to protein-coding genes (Figures 3B & S3). We similarly
488 assessed the Ribo-Zero depletion method for preservation of protein-coding RNA. Ribo-
489 Zero-treated libraries (R = 0.935-0.962) display a better correlation with the Unenriched
490 libraries than the Poly(A)-treated libraries, but a slightly weaker correlation than the
491 RNase H-treated libraries for reads mapping to protein-coding genes (Figure 3B & S3).
492 This observation demonstrates that the RNase H depletion method is more specific than
493 both the Poly(A) isolation and Ribo-Zero depletion methods in preserving protein-coding
494 RNA levels observed in the Unenriched RNA control libraries.
495
496 **RNase H depletion more accurately preserves true levels of ncRNA than Poly(A)**
497 **isolation, but slightly less accurately than Ribo-Zero depletion:**

We next assessed the ability of each RNA enrichment method to retain ncRNA specifically. To do so, we calculated the correlation coefficient between normalized reads mapped to ncRNA genes from all Unenriched RNA samples, in order to determine the maximum achievable correlation between libraries. Again, we observed that the Unenriched RNA samples are highly correlated (R = 0.835-0.990), demonstrating reproducibility between samples and batches (Figure 4A).

We compared the ability of the RNase H depletion method and the Poly(A) isolation method to preserve ncRNA following rRNA depletion. We calculated the correlation coefficient between normalized reads mapped to ncRNA genes in RNase H-treated/Poly(A)-treated libraries and normalized reads mapped to ncRNA genes from the Unenriched RNA control libraries. As expected, we found that the RNase H-treated libraries (R = 0.799-0.815) display a much better correlation with the Unenriched RNA control libraries than the Poly(A)-treated libraries (R = 0.139-0.149) for all reads mapping to ncRNA genes (Figures 4B & S4). This result was expected because the Poly(A) isolation method specifically enriches RNA with polyadenylation and excludes all other non-polyadenylated RNA, including ncRNA and tRNA. One key advantage of methods that specifically remove rRNA, such as the RNase H depletion and the Ribo-Zero depletion methods, is that they “ignore” all RNA that is not specifically targeted for removal. As a result, these non-polyadenylated RNA species should maintain similar levels as the input Unenriched RNA.

As a better assessment of the ability of the RNase H depletion method to preserve ncRNA, we compared it to the Ribo-Zero depletion method. Ribo-Zero-treated libraries (R = 0.897-0.967) display a slightly better correlation with the Unenriched

libraries than the RNase H-treated libraries for reads mapping to ncRNA genes (Figure 4B & S4). The higher correlation of Ribo-Zero-treated libraries with Unenriched libraries seems to be driven by CNAG_12993, the ncRNA gene with the highest counts in the Unenriched libraries, but much lower counts in the RNase H libraries. When CNAG_12993 is removed from analysis, the RNase H and Ribo-Zero depletion methods perform similarly (Figure S5; RNase H R = 0.936-0.952, Ribo-Zero R = 0.892-0.959). There is no clear explanation for the poor performance of the RNase H depletion method with CNAG_12993.

We also explored the ability of each enrichment method to preserve tRNA. Fewer than 10 reads mapped to each tRNA gene in all libraries, likely due to size selection in the library preparation, precluding any meaningful analysis (data not shown).

LncPipe pipeline identifies novel lncRNA in the *C. neoformans* transcriptome:

Because our correlation analyses demonstrated that both the RNase H depletion and the Ribo-Zero depletion methods preserve ncRNA, we took advantage of this rich RNA-Seq dataset to search for novel lncRNAs. We used an existing pipeline LncPipe (Zhao *et al.* 2018) that was developed for a subset of model organisms, and modified it for application to *C. neoformans*. We applied this modified LncPipe pipeline to identify novel lncRNA within our RNase H depletion, Ribo-Zero depletion, and Unenriched RNA datasets. Our lncRNA discovery analysis identified 11 novel lncRNA within the *C. neoformans* transcriptome (Table 1).

DISCUSSION

RNA enrichment is essential for cost-effectively generating data from an RNA-Seq experiment. We have demonstrated here that, in *C. neoformans* cells grown in rich media, rRNA constitutes more than 90% of the total RNA; even higher percentages of rRNA have been observed in other species (Giannoukos *et al.* 2012). RNA-Seq experiments are typically aimed at quantifying protein-coding RNA, and increasingly also ncRNA. Efficient reduction of rRNA allows one to generate the desired sequencing depth of the RNA species of interest with one-tenth of the sequencing reads that would be required to generate the same depth from total, unenriched RNA.

To be effective, RNA enrichment methods must be efficient and specific. An efficient RNA enrichment method removes as much rRNA as possible. A specific RNA enrichment method does not affect other RNA species in the sample. We compared the rRNA removal efficiency of three commonly-used methods in *C. neoformans* samples. Application of the RNase H depletion method in *Cryptococcus* has never been reported to our knowledge. The Poly(A) isolation method (Bloom *et al.* 2019; Brown *et al.* 2020) and the now discontinued Ribo-Zero depletion method have both been used in RNA-Seq applications with *Cryptococcus* samples in the past (Illumina; Trevijano-Contador *et al.* 2018; Liu *et al.* 2020). We find that both the untested RNase H depletion method, as well as the frequently-used Poly(A) selection method, are very efficient in removing fungal rRNA. Surprisingly, the Ribo-Zero depletion method showed poor efficiency in *C. neoformans*, despite previous work showing efficient removal of various bacterial rRNA (Giannoukos *et al.* 2012). While the Ribo-Zero manufacturer predicted that the Ribo-Zero Yeast kit would work for *C. neoformans*, the probes were designed to target *S. cerevisiae*, which may explain the poor performance observed here. Of the three

567 methods tested, the RNase H depletion method is the most efficient in removing fungal
568 rRNA.

569 Following the removal of rRNA, the majority of remaining RNA is typically protein-
570 coding. Ideally, the removal of rRNA should not have any effect on protein-coding RNA.
571 In reality, there is no known method that can reduce rRNA without having some effect
572 on non-target RNA, including protein-coding RNA. The best available methods
573 efficiently remove rRNA and are highly specific, having minimal side-effects on non-
574 target RNA. When assessing the ability of these RNA enrichment methods to preserve
575 protein-coding RNA, we observe that the RNase H depletion method is substantially
576 more specific than the Poly(A) isolation method and somewhat more specific than the
577 Ribo-Zero depletion method.

578 We evaluated the specificity of each RNA enrichment method in preserving
579 ncRNA. The Poly(A) isolation method performs very poorly in preserving ncRNA; this is
580 as expected since it depends on 3' polyadenylation, which is absent from ncRNA. The
581 RNase H depletion and the Ribo-Zero depletion methods both perform well in
582 preserving ncRNA, with the Ribo-Zero depletion method being slightly more specific
583 than the RNase H depletion method.

584 To determine a possible mechanism impacting specificity of the Poly(A) isolation
585 method, we identified the genes that were significantly underrepresented in the Poly(A)-
586 treated libraries compared to the Unenriched libraries (Figure S6). A total of 41 genes
587 were identified as significantly underrepresented in the Poly(A)-treated libraries; as
588 expected, 24 of these genes are non-coding genes (Table S1). In analyzing the
589 remaining 17 protein-coding genes that were underrepresented in the Poly(A)-treated

libraries, we observed a pattern. The vast majority of these genes (12 of 17) are located on the mitochondrial chromosome (Table S1). This observation is supported by previous work that has demonstrated that mitochondrial transcripts in fungi, including *Cryptococcus*, lack polyadenylation (Toffaletti *et al.* 2003; Chang and Tong 2012). From this analysis, it appears that the Poly(A) isolation method is largely specific for most protein-coding genes except for mitochondrial genes. We have not identified any characteristic that explains the five underrepresented protein coding genes that reside in the nuclear genome. These findings indicate that the Poly(A) isolation method is not well suited for RNA-Seq experiments investigating ncRNA genes, genes on the mitochondrial chromosome, or the five nuclear protein-coding genes that we found to be underrepresented in the Poly(A)-treated libraries.

Interest in ncRNA has recently expanded in the fungal genetics field. The majority of work has focused on ncRNAs in model systems (such as *S. cerevisiae, Neurospora crassa*, and *Aspergillus flavus*), in which lncRNAs and natural antisense transcripts (NATs) have been implicated in stress responses and development (Smith *et al.* 2008; Gelfand *et al.* 2011; Ding *et al.* 2012; Xue *et al.* 2014). Little work has explored ncRNAs in pathogenic fungi. For example, RNA interference (RNAi) is known to regulate transposon activity in *C. neoformans* (Wang *et al.* 2010; Janbon *et al.* 2010; Yadav *et al.* 2018). The first lncRNA in *Cryptococcus*, *RZE1*, was recently functionally characterized. *RZE1* is required for *Cryptococcus* yeast-to-hyphal transition and virulence through its regulation of the transcription factor *ZNF2* (Chacko *et al.* 2015). Additionally, siRNAs, miRNAs, and lncRNAs are known to be secreted, albeit for an unknown purpose, by *C. deneoformans* (Liu *et al.* 2020). We have identified 11 putative

lncRNAs in *C. neoformans* by mining our dataset by modifying LncPipe (Zhao *et al.* 2018) to run on genomic data from non-model organisms. Although many of these lncRNAs were not highly expressed in the evaluated condition, they may be interesting candidates to pursue for novel biological activity in conditions relevant to fungal pathogenesis, because many fungal ncRNAs are induced in response to stressful stimuli. Furthermore, the *C. neoformans* genome may contain undiscovered lncRNAs that are not expressed in the rich growth conditions used here.

In conclusion, of the three RNA enrichment methods compared here, we consider the Poly(A) isolation method to have poor overall effectiveness. It does efficiently reduce rRNA reads (although not as efficiently as the RNase H depletion method), but it results in a biased enrichment of protein-coding transcripts. The RNase H depletion and the Ribo-Zero depletion methods both display strengths and weaknesses. The RNase H depletion method performs better in efficiency of rRNA reduction and specificity for protein-coding transcripts, while the Ribo-Zero depletion method performs moderately better in specificity for ncRNA. While this work was being conducted, the Ribo-Zero product line was discontinued. It has since been replaced with the Illumina Ribo-Zero Plus rRNA Depletion Kit, which only targets human, mouse, rat, and bacterial rRNA. As a result, we conclude that the RNase H method may be the best option for RNA-Seq analysis of *C. neoformans*, as well as many other non-model organisms. While the RNase H depletion method has a substantial upfront cost to purchase DNA oligonucleotides (approximately $1000), we estimate that for this method our total cost per sample was less than $6.50 (more than half of this total was the final cleanup with the Zymo RNA Clean & Concentrator-5 kit).

636

637 ## ACKNOWLEDGEMENTS

638 We thank the Duke University School of Medicine for the use of the Microbiome
639 Shared Resource, which provided RNA quality assessments. We also thank the Duke
640 University School of Medicine for the use of the Sequencing and Genomic Technologies
641 Shared Resource, which provided all sequencing services used for this project. This
642 work was made possible by funding from the National Institute of Biomedical Imaging
643 and Bioengineering (grant #5R25EB023928) received by KO and CC, and R01 grant
644 AI074677 to JAA and JAG.

645

646 ## FIGURE LEGENDS

647 **Figure 1. rRNA depletion efficiency:** The percentage of rRNA reads in each library is
648 graphed. The RNase H depletion method has the most efficient depletion (lowest
649 percentage of rRNA reads), with the Poly(A) isolation method a close second, and the
650 Ribo-Zero depletion method a distant third. Unenriched libraries show that rRNA makes
651 up most of the RNA in *C. neoformans*.

652

653 **Figure 2. Specificity of rRNA depletion for all genes:** Pearson correlations were
654 calculated for normalized read counts of all annotated genes in the *C. neoformans*
655 genome, excluding rRNA genes and genes containing coding-strand rRNA duplications.
656 A. Unenriched libraries have high internal consistency as determined by leave-one-out
657 cross correlation of each Unenriched library with the mean of other Unenriched libraries.
658 B. The RNase H depletion method has the best overall rRNA depletion specificity, as

659 determined by Pearson correlation of read counts for all genes with the Unenriched
660 libraries. Pearson correlation coefficient (R) was calculated between each enriched
661 library and the gold standard, the gene-wise average of counts across all Unenriched
662 library replicates.
663
664 **Figure 3. Specificity of rRNA depletion for protein-coding genes:** Pearson
665 correlations were calculated in the same way as Figure 2, but only for protein-coding
666 genes, excluding genes containing coding-strand rRNA duplications. A. Unenriched
667 libraries have high internal consistency for protein-coding genes. B. The RNase H
668 depletion method has the best rRNA depletion specificity for protein-coding genes.
669
670 **Figure 4. Specificity of rRNA depletion for ncRNA genes:** Pearson correlations were
671 calculated in the same way as Figure 2, but only for ncRNA genes, excluding rRNA
672 genes. A. Unenriched libraries have high internal consistency for ncRNA genes. B. The
673 Ribo-Zero depletion method has the best rRNA depletion specificity for ncRNA genes.
674
675 **TABLE LEGEND**
676 **Table 1. LncPipe identification of novel *C. neoformans* lncRNA:** Putative lncRNAs
677 were discovered by analysis of RNase H-treated, Ribo-Zero-treated, and Unenriched
678 RNA libraries. The name (assigned by LncPipe), chromosomal location, exon number,
679 exonic length, and transcripts per million (TPM) across samples are shown for all 11
680 novel lncRNA identified.
681

682 # SUPPLEMENTARY MATERIAL

683 **Figure S1. Visualization of mitochondrial rRNA genes in *C. neoformans* H99**
684 **strain:** The depth of coverage plot of the whole H99 mitochondrial chromosome is
685 shown. The *C. neoformans* large and small mitochondrial rRNA genes are clearly
686 identified as the two regions of the mitochondrial genome with depth of coverage that is
687 much higher than any other part of the chromosome.

688

689 **Figure S2. Scatterplot visualization of rRNA depletion specificity for all genes:** In
690 the RNase H- and Ribo-Zero-treated libraries, most genes have counts that are highly
691 correlated with the Unenriched libraries, whereas Poly(A)-treated libraries have low
692 counts for a number of expressed genes. For each biological replicate (subplot columns
693 labeled “A”, “B”, and “C”), per-gene normalized read counts for each enrichment method
694 are plotted as a function of the gold standard (normalized read counts averaged across
695 the Unenriched libraries). All annotated genes in the *C. neoformans* genome are
696 plotted, excluding rRNA genes and genes containing coding-strand rRNA duplications.
697 For libraries with technical replicates (RNase H and Ribo-Zero), only one of the
698 replicates is shown.

699

700 **Figure S3. Scatterplot visualization of rRNA depletion specificity for protein-**
701 **coding genes:** In the RNase H- and Ribo-Zero-treated libraries, most protein-coding
702 genes have counts that are highly correlated with the Unenriched libraries, whereas
703 Poly(A)-treated libraries have low counts for a number of protein-coding genes. This plot

is the same as Figure S2, but only shows protein-coding genes, excluding genes containing coding-strand rRNA duplications.

Figure S4. Scatterplot visualization of rRNA depletion specificity for ncRNA genes: In the RNase H- and Ribo-Zero-treated libraries, most ncRNA genes have counts that are well-correlated with the Unenriched libraries, whereas Poly(A)-treated libraries have low counts for almost all ncRNA genes. This plot is the same as Figure S2, but only shows ncRNA genes, excluding rRNA.

Figure S5. Specificity of rRNA depletion for ncRNA genes, excluding CNAG_12993: When outlier ncRNA gene CNAG_12993 is excluded, the RNase H depletion method has specificity for ncRNA genes that is as good as the Ribo-Zero depletion method. Pearson correlations were calculated in the same way as Figure 4, except CNAG_12993 was excluded from the analysis.

Figure S6. Scatterplot visualization of all genes underrepresented by the Poly(A) isolation method: This plot is the same as Figure S2, with the genes that are significantly underrepresented in the Poly(A)-treated libraries colored red.

Table S1. Genes underrepresented by the Poly(A) isolation method: Table details the genes that are significantly underrepresented in the Poly(A)-treated libraries. The gene name, chromosome, and gene type are included for each gene.

File S1. RNase H depletion protocol: The detailed protocol used to perform the RNase H depletion.

File S2. Ensembl GTF with newly annotated mitochondrial rRNA: A copy of the GTF genome annotation file for CNA3 of H99 *Cryptococcus neoformans* var. *grubii*, modified to include annotation for the mitochondrial rRNA genes.

File S3. RNase H rRNA-targeting oligonucleotides: DNA oligonucleotide sequences used in the RNase H depletion method to target H99 *C. neoformans* rRNA. This file was formatted to be directly pasted into the Eurofins order form.

LITERATURE CITED

Adiconis, X., D. Borges-Rivera, R. Satija, D. S. Deluca, M. A. Busby *et al.*, 2013 Comparative analysis of RNA sequencing methods for degraded or low-input samples. Nat. Methods. 10: 623–629.

Altschul, S. F., W. Gish, W. Miller, E. W. Myers, and D. J. Lipman, 1990 Basic local alignment search tool. J. Mol. Biol. 215: 403–410.

Andrews, S., 2010 FastQC: A quality control tool for high throughput sequence data. Available online at: http://www.bioinformatics.babraham.ac.uk/projects/fastqc/.

Aronesty, E., 2011 ea-utils : Command-line tools for processing biological sequencing data. Available online at: http://expressionanalysis.github.io/ea-utils/.

Atkinson, S. R., S. Marguerat, D. A. Bitton, M. Rodríguez-López, C. Rallis *et al.*, 2018 Long noncoding RNA repertoire and targeting by nuclear exosome, cytoplasmic

exonuclease, and RNAi in fission yeast. RNA 24: 1195–1213.

Barrett, T., S. E. Wilhite, P. Ledoux, C. Evangelista, I. F. Kim *et al.*, 2013 NCBI GEO: Archive for functional genomics data sets - Update. Nucleic Acids Res. 41: D991–D995.

Bird, A. J., M. Gordon, D. J. Eide, and D. R. Winge, 2006 Repression of *ADH1* and *ADH3* during zinc deficiency by Zap1-induced intergenic RNA transcripts. EMBO J. 25: 5726–5734.

Bloom, A. L. M., R. M. Jin, J. Leipheimer, J. E. Bard, D. Yergeau *et al.*, 2019 Thermotolerance in the pathogen *Cryptococcus neoformans* is linked to antigen masking via mRNA decay-dependent reprogramming. Nat. Commun. 10: 1–13.

Brown, H. E., K. S. Ost, S. K. Esher, K. M. Pianalto, J. W. Saelens *et al.*, 2018 Identifying a novel connection between the fungal plasma membrane and pH-sensing. Mol. Microbiol. 109: 474–493.

Brown, H. E., C. L. Telzrow, J. W. Saelens, L. Fernandes, and J. A. Alspaugh, 2020 Sterol-response pathways mediate alkaline survival in diverse fungi. mBio 11: e00719-20.

Bumgarner, S. L., R. D. Dowell, P. Grisafi, D. K. Gifford, and G. R. Fink, 2009 Toggle involving cis-interfering noncoding RNAs controls variegated gene expression in yeast. Proc. Natl. Acad. Sci. U. S. A. 106: 18321–18326.

Bumgarner, S. L., G. Neuert, B. F. Voight, A. Symbor-Nagrabska, P. Grisafi *et al.*, 2011 Single-cell analysis reveals that noncoding RNAs contribute to clonal heterogeneity by modulating transcription factor recruitment. Mol. Cell 45: 470–482.

Chacko, N., Y. Zhao, E. Yang, L. Wang, J. J. Cai *et al.*, 2015 The lncRNA *RZE1*

773 controls cryptococcal morphological transition. PLoS Genet. 11: e1005692.
774 Chang, Y. C., A. K. Lamichhane, H. M. Garraffo, P. J. Walter, and M. Leerkes, 2014
775 Molecular mechanisms of hypoxic responses via unique roles of Ras1, Cdc24 and
776 Ptp3 in a human fungal pathogen *Cryptococcus neoformans*. PLoS Genet. 10:
777 e1004292.
778 Chang, J. H., and L. Tong, 2012 Mitochondrial poly(A) polymerase and polyadenylation.
779 Biochim. Biophys. Acta 1819: 992–997.
780 Chen, Y., D. L. Toffaletti, J. L. Tenor, A. P. Litvintseva, C. Fang *et al.*, 2014 The
781 *Cryptococcus neoformans* transcriptome at the site of human meningitis. mBio 5:
782 e01087-13.
783 Chow, E. W. L., S. A. Clancey, R. Blake Billmyre, A. F. Averette, J. A. Granek *et al.*,
784 2017 Elucidation of the calcineurin-Crz1 stress response transcriptional network in
785 the human fungal pathogen *Cryptococcus neoformans*. PLoS Genet. 13: e1006667.
786 Ding, D. Q., K. Okamasa, M. Yamane, C. Tsutsumi, T. Haraguchi *et al.*, 2012 Meiosis-
787 specific noncoding RNA mediates robust pairing of homologous chromosomes in
788 meiosis. Science 336: 732–736.
789 Dobin, A., C. A. Davis, F. Schlesinger, J. Drenkow, C. Zaleski *et al.*, 2013 STAR:
790 Ultrafast universal RNA-seq aligner. Bioinformatics 29: 15–21.
791 Edgar, R., M. Domrachev, and A. E. Lash, 2002 Gene Expression Omnibus: NCBI gene
792 expression and hybridization array data repository. Nucleic Acids Res. 30: 207–
793 210.
794 Ewels, P., M. Magnusson, S. Lundin, and M. Käller, 2016 MultiQC: Summarize analysis
795 results for multiple tools and samples in a single report. J. Bioinform. 32: 3047–

3048.

Fan, W., P. R. Kraus, M. J. Boily, and J. Heitman, 2005 *Cryptococcus neoformans* gene expression during murine macrophage infection. Eukaryot. Cell 4: 1420–1433.

Gelfand, B., J. Mead, A. Bruning, N. Apostolopoulos, V. Tadigotla *et al.*, 2011 Regulated antisense transcription controls expression of cell-type-specific genes in yeast. Mol. Cell. Biol. 31: 1701–1709.

Giannoukos, G., D. M. Ciulla, K. Huang, B. J. Haas, J. Izard *et al.*, 2012 Efficient and robust RNA-seq process for cultured bacteria and complex community transcriptomes. Genome Biol. 13: r23.

Gish, S. R., E. J. Maier, B. C. Haynes, F. H. Santiago-Tirado, D. L. Srikanta *et al.*, 2016 Computational analysis reveals a key regulator of cryptococcal virulence and determinant of host response. mBio 7: e00313-16.

Hazkani-Covo, E., R. M. Zeller, and W. Martin, 2010 Molecular poltergeists: Mitochondrial DNA copies (numts) in sequenced nuclear genomes. PLoS Genet. 6: e1000834.

Illumina. Ribo-Zero Kit Species Compatibility Tables. Available online at: https://www.tst-web.illumina.com/content/illumina-marketing/amr/en/products/selection-tools/ribo-zero-kit-species-compatibility.html.

Isenbarger, T. A., C. E. Carr, S. S. Johnson, M. Finney, G. M. Church *et al.*, 2008 The most conserved genome segments for life detection on earth and other planets. Orig. Life Evol. Biosph. 38: 517–533.

Janbon, G., S. Maeng, D. H. Yang, Y. J. Ko, K. W. Jung *et al.*, 2010 Characterizing the role of RNA silencing components in *Cryptococcus neoformans*. Fungal Genet.

819 Biol. 47: 1070–1080.

820 Janbon, G., K. L. Ormerod, D. Paulet, E. J. Byrnes, V. Yadav *et al.*, 2014 Analysis of the
821 genome and transcriptome of *Cryptococcus neoformans* var. *grubii* reveals
822 complex RNA expression and microevolution leading to virulence attenuation.
823 PLoS Genet. 10: e1004261.

824 Jiang, N., Y. Yang, G. Janbon, J. Pan, and X. Zhu, 2012 Identification and functional
825 demonstration of miRNAs in the fungus *Cryptococcus neoformans*. PLOS One 7:
826 e52734.

827 Kersey, P. J., J. E. Allen, I. Armean, S. Boddu, B. J. Bolt *et al.*, 2016 Ensembl Genomes
828 2016: More genomes, more complexity. Nucleic Acids Res. 44: D574–D580.

829 Liu, M., Z. Zhang, C. Ding, T. Wang, B. Kelly *et al.*, 2020 Transcriptomic analysis of
830 extracellular RNA governed by the endocytic adaptor protein Cin1 of *Cryptococcus*
831 *deneoformans*. Front. Cell. Infect. Microbiol. 10: 256.

832 Morlan, J. D., K. Qu, and D. V. Sinicropi, 2012 Selective depletion of rRNA enables
833 whole transcriptome profiling of archival fixed tissue. PLOS One 7: e42882.

834 Parker, S., M. G. Fraczek, J. Wu, S. Shamsah, A. Manousaki *et al.*, 2018 Large-scale
835 profiling of noncoding RNA function in yeast. PLoS Genet. 14: e1007253.

836 Rajasingham, R., R. M. Smith, B. J. Park, J. N. Jarvis, N. P. Govender *et al.*, 2017
837 Global burden of disease of HIV-associated cryptococcal meningitis: an updated
838 analysis. Lancet Infect. Dis. 17: 873–881.

839 Smith, C. A., D. Robertson, B. Yates, D. M. Nielsen, D. Brown *et al.*, 2008 The effect of
840 temperature on Natural Antisense Transcript (NAT) expression in *Aspergillus*
841 *flavus*. Curr. Genet. 54: 241–269.

Toffaletti, D. L., M. Del Poeta, T. H. Rude, F. Dietrich, and J. R. Perfect, 2003 Regulation of cytochrome c oxidase subunit 1 (*COX1*) expression in *Cryptococcus neoformans* by temperature and host environment. Microbiology 149: 1041–1049.

Trevijano-Contador, N., H. C. de Oliveira, R. García-Rodas, S. A. Rossi, I. Llorente *et al.*, 2018 *Cryptococcus neoformans* can form titan-like cells in vitro in response to multiple signals. PLoS Pathog. 14: e1007007.

Wang, X., Y. P. Hsueh, W. Li, A. Floyd, R. Skalsky *et al.*, 2010 Sex-induced silencing defends the genome of *Cryptococcus neoformans* via RNAi. Genes Dev. 24: 2566–2582.

Xue, Z., Q. Ye, S. R. Anson, J. Yang, G. Xiao *et al.*, 2014 Transcriptional interference by antisense RNA is required for circadian clock function. Nature 514: 650–653.

Yadav, V., S. Sun, R. B. Billmyre, B. C. Thimmappa, T. Shea *et al.*, 2018 RNAi is a critical determinant of centromere evolution in closely related fungi. Proc. Natl. Acad. Sci. U. S. A. 115: 3108–3113.

Yi, H., Y.-J. Cho, S. Won, J.-E. Lee, H. J. Yu *et al*., 2011 Duplex-specific nuclease efficiently removes rRNA for prokaryotic RNA-seq. Nucleic Acids Res. 39: e140.

Yu, C.-H., Y. Chen, C. A. Desjardins, J. L. Tenor, D. L. Toffaletti *et al.*, 2020 Landscape of gene expression variation of natural isolates of *Cryptococcus neoformans* in response to biologically relevant stresses. Microb. Genomics 6.

Zhao, W., X. He, K. A. Hoadley, J. S. Parker, D. N. Hayes *et al.*, 2014 Comparison of RNA-Seq by poly (A) capture, ribosomal RNA depletion, and DNA microarray for expression profiling. BMC Genomics 15: 419.

Zhao, Q., Y. Sun, D. Wang, H. Zhang, K. Yu *et al.*, 2018 LncPipe: A Nextflow-based

865 pipeline for identification and analysis of long non-coding RNAs from RNA-Seq

866 data. J. Genet. Genomics 45: 399–401.

867

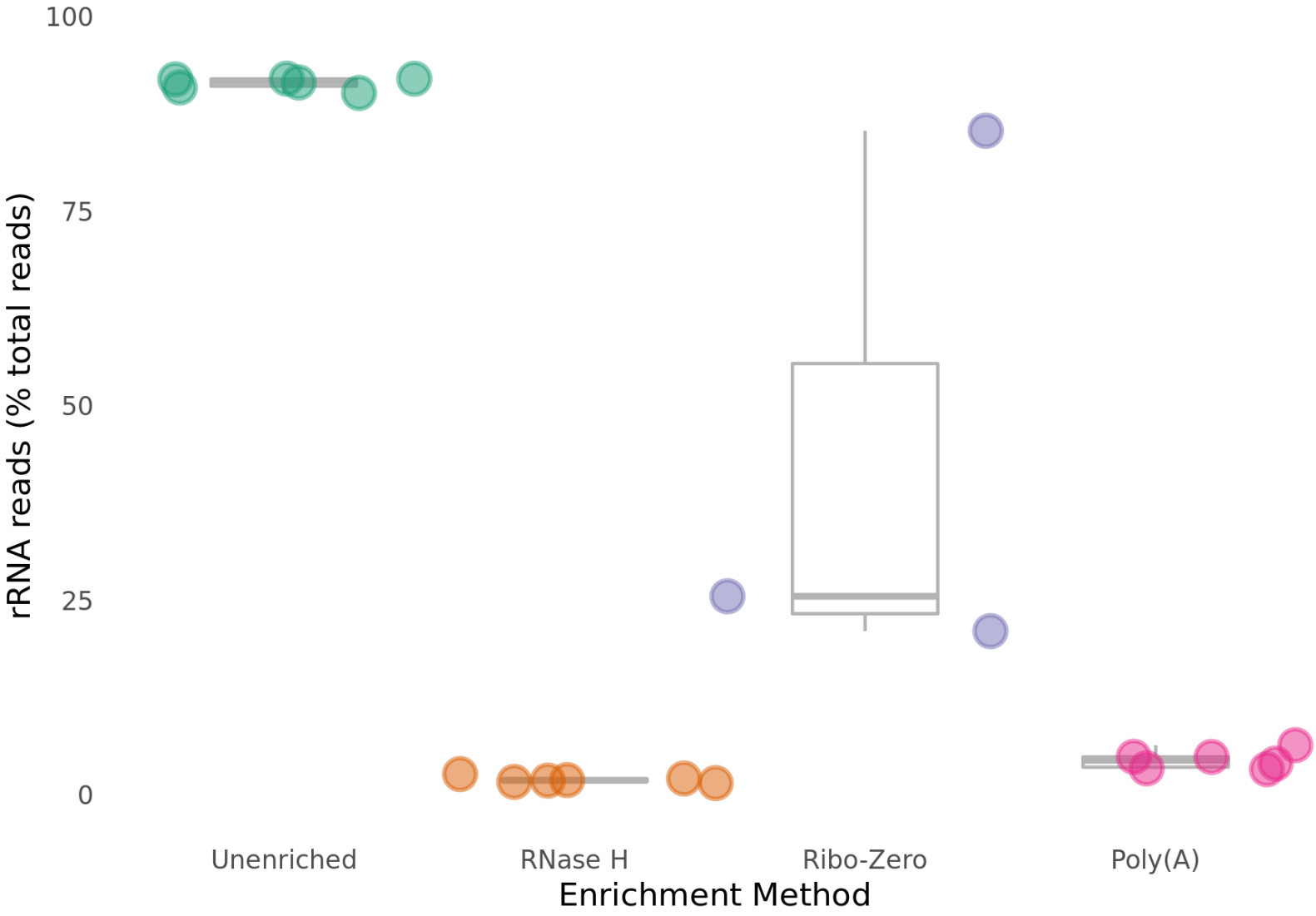

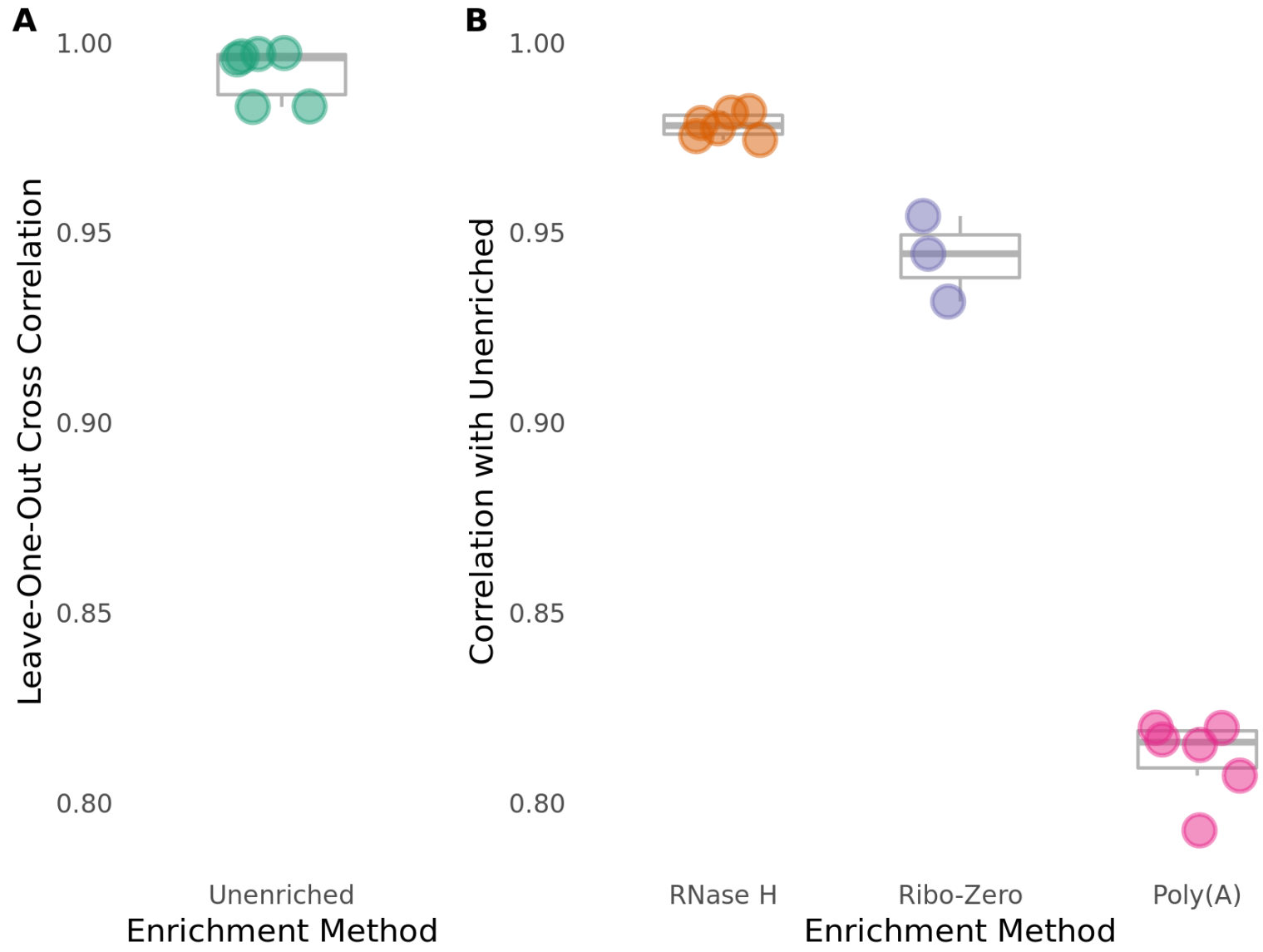

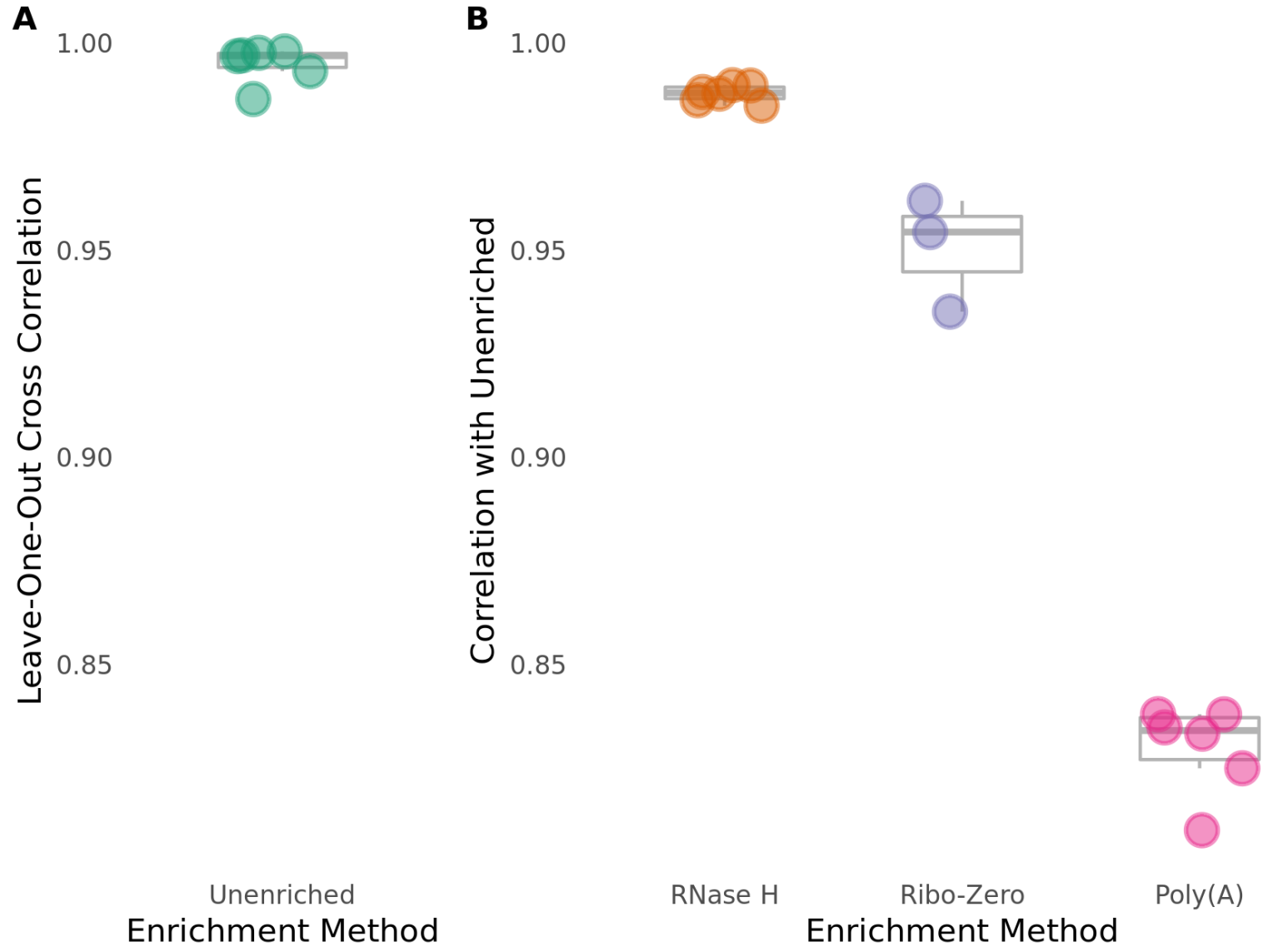

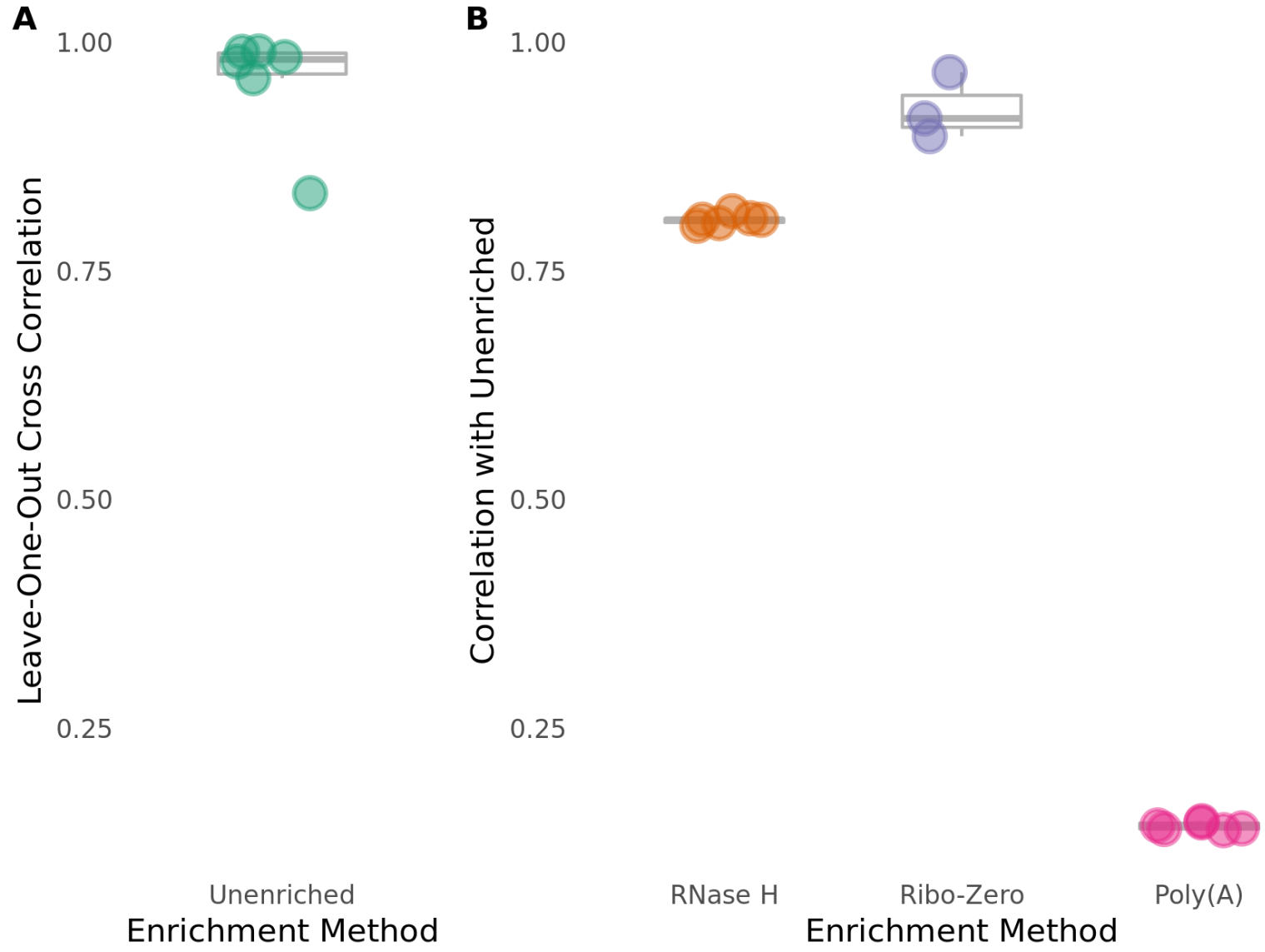

Table 1. LncPipe identification of novel *C. neoformans* lncRNA:

Name	Chromosome	Start	End	# Exons	Total Exonic Length	Mean TPM	Median TPM
LINC-CNAG_07358-1	1	996421	997387	2	863	6.689427833	6.2667
LINC-CNAG_07633-1	6	499352	499840	3	350	2.844233167	0
LINC-CNAG_07649-1	6	1351673	1352718	3	913	5.5161474	5.799715
LINC-CNAG_07769-5	9	828268	829327	3	919	9.2005976	10.76355
LINC-CNAG_07769-4	9	831951	833064	4	2019	5.333811583	5.026716
LINC-CNAG_07769-1	9	838389	840007	10	2730	4.443440783	3.846055
LINC-CNAG_04857-1	10	199988	203380	43	6849	12.5665295	12.729905
LINC-CNAG_04857-2	10	203693	205767	2	1983	1.903616517	1.67792
LINC-CNAG_01945-1	11	1333989	1334590	2	540	3.47618165	1.745465
LINC-CNAG_06521-2	13	743402	744570	4	1003	5.924291983	5.627535
LINC-CNAG_07042-1	13	750280	751009	3	609	5.950332833	4.02392

Table 1. LncPipe identification of novel *C. neoformans* lncRNA: Putative lncRNAs were discovered by analysis of RNase H-treated, Ribo-Zero-treated, and Unenriched RNA libraries. The name (assigned by LncPipe), chromosomal location, exon number, exonic length, and transcripts per million (TPM) across samples are shown for all 11 novel lncRNA identified.